

Probing dephasing and non-Markovian effects on three-qubit states

Muhammad Noman, Aqsa Mushtaq, and Wei Cui(崔巍)
Citation: Chin. Phys. B, 2026, 35 (**5**): 050302. DOI: 10.1088/1674-1056/ae1822
http://cpb.iphy.ac.cn; http://iopscience.iop.org/cpb

What follows is a list of articles you may be interested in

Measurement-device-independent quantum key distribution with entanglement-assisted linear Bell state measurement

Cheng Zhang(张诚), Cheng Liu(刘成), Jiawei Ying(应佳伟), Shipu Gu(顾世浦), Lan Zhou(周澜), Yin Ma(马寅), Kang Gao(高亢), Hai Wei(魏海), Kai Wen(文凯), and Yubo Sheng(盛宇波)
Chin. Phys. B, 2026, 35 (**4**): 040310. DOI: 10.1088/1674-1056/ae3605

Geometric control of concurrence and quantum gate operations in triangular triple quantum dots

Junqing Li(李俊青), Shuo Dong(董硕), and Jianhua Wei(魏建华)
Chin. Phys. B, 2026, 35 (**2**): 020302. DOI: 10.1088/1674-1056/adec5d

Unveiling the physical meaning of transformer attention in neural network quantum states: A conditional mutual information perspective

Tianyu Ruan(阮天雨), Bowen Kan(阚博文), Yixuan Sun(孙艺轩), Honghui Shang(商红慧), Shihua Zhang(张世华), and Jinlong Yang(杨金龙)
Chin. Phys. B, 2026, 35 (**1**): 010301. DOI: 10.1088/1674-1056/ae1118

Quantum-enhanced time-of-arrival measuring method based on partially entangled state

Peng-Xian Li(李芃鲜), Lu-Ping Xu(许录平), Gui-Ting Hu(胡桂廷), and Wen-Long Gao(高文珑)
Chin. Phys. B, 2025, 34 (**7**): 070303. DOI: 10.1088/1674-1056/adc7ee

Measurement-based entanglement purification for hybrid entangled state

Cheng-Chen Luo(罗程晨), Shi-Pu Gu(顾世浦), Xing-Fu Wang(王兴福), Lan Zhou(周澜), and Yu-Bo Sheng(盛宇波)
Chin. Phys. B, 2025, 34 (**3**): 030307. DOI: 10.1088/1674-1056/adb267

Probing dephasing and non-Markovian effects on three-qubit states

Muhammad Noman[1], Aqsa Mushtaq[2], and Wei Cui(崔巍)[1,3,†]

[1] *School of Automation Science and Engineering, South China University of Technology, Guangzhou* 510641, *China*
[2] *Center for High Energy Physics, University of the Punjab, Lahore* 54590, *Pakistan*
[3] *Quantum Science Center of Guangdong–Hong Kong–Macau Greater Bay Area, Shenzhen* 518000, *China*

(Received 30 September 2025; revised manuscript received 27 October 2025; accepted manuscript online 28 October 2025)

We investigate the dynamical maps of coherence, entanglement, and purity in two distinct three-qubit class states: the Werner (W-like) and Greeneberger–Horne–Zeillinger (GHZ-like) states. Utilizing a classical channel affected by Ornstein Uhlenbeck (OU) and Random Telegraph (RT) noise, we explore two scenarios: coupling two qubits with RT noise and one with OU noise, and *vice versa*. The preservation of coherence, entanglement, and purity is analyzed using the ℓ_1 norm of coherence, entanglement witness operation, and purity measures. Our results reveal that the considered dephasing channels lead to a decrease in initially encoded quantum correlations, even in the presence of Gaussian OU noise, which typically induces monotonic decay. The non-monotonic behavior and decay are primarily governed by the parameters of OU and RT noises, with the configuration where OU noise affects two qubits and RT noise affects the third being optimal for quantum correlation preservation. Comparing the two states, the GHZ-like state exhibits superior preservation under RT noise influencing two local fields and qubits, while the W-like state performs better when OU noise affects two qubits. Overall, the GHZ-like state shows enhanced revival characteristics compared to the W-like state.

Keywords: entanglement, coherence, purity, Markovian/non-Markovian maps, GHZ-/W-like state

PACS: 03.65.Yz

DOI: 10.1088/1674-1056/ae1822 **CSTR:** 32038.14.CPB.ae1822

1. Introduction

Quantum technologies, including quantum computing, secure communication, and high precision metrology, rely on the preservation and control of quantum correlations such as coherence and entanglement.[1,2] These correlations enable quantum systems to outperform their classical counterparts in computational efficiency and cryptographic security. However, in practical implementations, quantum states inevitably interact with their surrounding environment, leading to decoherence and the degradation of quantum resources.[3] One of the most significant forms of decoherence arises from classical dephasing noise, which stems from random fluctuations in external fields that couple to the system.[4] Understanding the effects of such noise on multipartite quantum states is crucial for developing robust quantum information protocols capable of maintaining quantum coherence and entanglement over extended durations.[5] In this context, non-Markovian noise models such as the Ornstein Uhlenbeck (OU) and Random Telegraph (RT) processes have received considerable attention due to their ability to capture memory effects and stochastic fluctuations that influence quantum dynamics.[6,7] Investigating how quantum correlations evolve under the influence of these noise models provides valuable insights into the fundamental limitations and practical possibilities of quantum technologies in realistic noisy environments.[8]

Among multipartite quantum states, three-qubit entangled states play a fundamental role in quantum information processing, quantum error correction, and distributed quantum networks.[9,10] In particular, the Greenberger–Horne–Zeilinger (GHZ) and W-states are two distinct representatives of three-qubit entanglement classes, each exhibiting unique properties when subjected to environmental noise.[11] The GHZ state is highly sensitive to decoherence but remains an essential resource for quantum cryptographic protocols, fault-tolerant quantum computation, and nonlocality tests.[12] In contrast, the W state, while not maximally entangled in the same way as the GHZ state, is known for its robustness against specific types of noise and decoherence, making it advantageous for tasks requiring entanglement preservation.[13,14] Despite their fundamental differences, the behavior of these states under mixed dephasing noise, particularly when influenced by both OU and RT processes, remains an open question with significant implications for quantum error mitigation and information processing. In this work, we systematically examine the coherence, entanglement, and purity of GHZ and W-like states under different noise configurations, revealing the intricate ways in which classical dephasing affects multipartite quantum systems.[15] Our findings provide a deeper understanding of noise induced effects in three-qubit states and highlight optimal conditions for preserving quantum correlations in practical implementations.[16,17]

Coherence is a fundamental property of quantum systems

†Corresponding author. E-mail: aucuiwei@scut.edu.cn

© 2026 Chinese Physical Society and IOP Publishing Ltd. All rights, including for text and data mining, AI training, and similar technologies, are reserved.

that arises from the superposition principle.[18] It quantifies the ability of a quantum state to exhibit interference effects,[19] which are essential for quantum information processing tasks such as quantum computing and cryptography.[20,21] In tripartite systems, coherence is particularly significant in states like the GHZ and W-states.[22] The GHZ-state exhibits global coherence, meaning it is highly sensitive to decoherence in any of its qubits.[23] On the other hand, the W-state demonstrates a more distributed form of coherence, as it retains some coherence even when one qubit is lost or measured.[24] This difference makes the W-state more robust against certain types of decoherence compared to the GHZ-state.[25] Besides coherence, entanglement is a non-classical correlation between subsystems of a quantum state and is a key resource for quantum information processing.[26] In tripartite systems, the GHZ-state is a prime example of genuine tripartite entanglement, where the entanglement is shared collectively among all three qubits.[27] If any one qubit is traced out, the remaining two qubits become separable, highlighting the fragility of GHZ entanglement.[28] In contrast, the W-state exhibits pairwise entanglement, meaning that when one qubit is traced out, the remaining two qubits remain entangled.[29] This makes the W-state more resilient to particle loss and decoherence, making it suitable for applications requiring robustness.[30] Moreover, purity measures the degree of mixedness in a quantum state. For pure states like the GHZ and W-states, the purity is maximal, meaning they are perfectly coherent and entangled.[31] However, in practical scenarios, these states may become mixed due to interactions with the environment or imperfect preparation.[32] The GHZ-state, being highly sensitive to decoherence, can quickly lose its purity, leading to a mixed state with reduced coherence and entanglement.[33] The W-state, due to its distributed entanglement, tends to retain higher purity under similar conditions, making it more suitable for applications in noisy environments.[34]

Classical dephasing noises, such as Ornstein–Uhlenbeck (OU) and Random Telegraph (RT) noises, have a significant impact on the dynamics of tripartite quantum states.[35] OU noise is characterized by a Gaussian correlation function and causes a gradual decay of coherence and entanglement over time.[33] RT noise, on the other hand, switches between discrete values and leads to sudden jumps in coherence and entanglement.[35] These noises affect the GHZ and W-states differently due to their distinct entanglement structures. The GHZ-state, with its global coherence and tripartite entanglement, is highly susceptible to both OU and RT noises, leading to rapid decoherence and loss of entanglement.[33] The W-state, with its distributed coherence and pair wise entanglement, is more resilient and retains some coherence and entanglement even under noisy conditions.[34] However, mixing OU and RT noises is crucial for studying the dynamics of tripartite quantum states because real world environments often exhibit a combination of both gradual and sudden noise processes.[35] OU noise models environments with continuous fluctuations, such as thermal noise, while RT noise models environments with discrete jumps, such as switching defects in solid state systems.[36] By combining these noises, we can more accurately capture the complex decoherence dynamics of quantum systems. For tripartite states like the GHZ and W-states, mixed noise can reveal interesting interplay between gradual and sudden decoherence processes. For instance, the GHZ state may experience rapid initial decoherence due to RT noise, followed by a slower decay due to OU noise.[33] The W-state, due to its resilience, may exhibit a more gradual decline in coherence and entanglement under mixed noise.[34] Understanding these dynamics is essential for designing robust quantum information protocols in realistic noisy environments.[35]

In this work, we present a mixture state which combines the GHZ and W-type states exposing it to an external classical field. Besides, no external environment imposed for the quantum information processing is realistically free of dephasing, therefore, two non matching noises, namely, the Gaussian/OU[37] and non-Gaussian/non-Markovian RT noise[38] are considered influencing the configuration. The first is caused by the random motion of the transmitting channel and the second place is caused by the interaction of the system with the charges at surface of the classical channel. For the entanglement quantification, we aim to employ entanglement witness, for coherence, we will use the ℓ_1-norm of coherence. It will be also interesting to see how much the system remains pure under the external classical dephasing limits, hence, we use purity to measure the pureness of the quantum state. In short, this study is significant in quantum information and computing, as it investigates the interplay between quantum coherence, entanglement, and noise in a three-qubit system. By exploring the effects of mixed OU and RT noise on quantum correlations, the study provides critical insights into the robustness and fragility of quantum states, particularly W-class and GHZ-class states. The use of realistic noise models like OU and RT noise is crucial for understanding decoherence in practical quantum computing protocols, where environmental interactions often degrade quantum resources.

This work is designed as; In Section 2, the physical model and dynamics of the system are given in detail. Section 3 provides an insight into the major results obtained and in the final Section 4, we summarize our study.

2. Physical model

A system with three qubits that was initially developed as a combined state of W-class and GHZ-class states that were subjected to mixed OU and RTN local fields. We considered examining the mixed fields in two situations: in the first case,

we couple the three-qubit state with two RTN noisy and one OU noisy field. In the second place, two OU noises and one RTN noise field are employed for the dynamics of the three-qubit state. The current physical model is governed by the Hamiltonian illustrated as[39]

$$H_{abc}(t) = H_a(t)\otimes \boldsymbol{I}_b\otimes \boldsymbol{I}_c + \boldsymbol{I}_a\otimes H_b(t)\otimes \boldsymbol{I}_c + \boldsymbol{I}_a\otimes \boldsymbol{I}_b\otimes H_c(t), \tag{1}$$

with $i=\{a,b,c\}$ in the above equation, $H_n(t)=E\boldsymbol{I}+\mathcal{L}\mathcal{D}_n(t)\sigma_z$ is the Hamiltonian of sub-system n, equal energy splitting is assumed to be E, $\boldsymbol{I}$ is the identity matrix, $1\geq \mathcal{D}_n(t)\geq -1$ in the given range denotes the stochastic component, $\mathcal{L}$ is linking strength between qubit-field, and σ_z denotes the Pauli matrix both of order 2×2. Time evolution of the state is[39]

$$\rho_{abc}(t)=U_{abc}(t)\rho_{\rm o}U_{abc}(t)^{\dagger}, \tag{2}$$

where the time evolution operator is formally expressed as

$$U_{abc}(t)=\mathcal{T}\exp\left[-\mathrm{i}\int_{t_0}^{t}H_{abc}(s)\,\mathrm{d}s\right]. \tag{3}$$

Here $\hbar=1$ with $\rho_{\rm o}$ being the initial density matrix given by[40]

$$\rho_{\rm o}=(1-p)\rho_{\rm GHZ}+p(\rho_{\rm W}), \tag{4}$$

where $0\leq p\leq 1$ and $\rho_{\rm GHZ}=|GHZ\rangle\langle GHZ|$ while $\rho_{\rm W}=|W\rangle\langle W|$ with $|GHZ\rangle=\frac{1}{\sqrt{2}}(|000\rangle+|111\rangle)$, and $|W\rangle=\frac{1}{\sqrt{3}}(|001\rangle+|010\rangle+|100\rangle)$ denotes the maximally entangled GHZ- and W-like states. The explicit initial matrices of the system are written as

$$\rho_{\rm GHZ}=\begin{bmatrix} 1/2 & 0 & 0 & 0 & 0 & 0 & 0 & 1/2\\ 0 & 0 & 0 & 0 & 0 & 0 & 0 & 0\\ 0 & 0 & 0 & 0 & 0 & 0 & 0 & 0\\ 0 & 0 & 0 & 0 & 0 & 0 & 0 & 0\\ 0 & 0 & 0 & 0 & 0 & 0 & 0 & 0\\ 0 & 0 & 0 & 0 & 0 & 0 & 0 & 0\\ 0 & 0 & 0 & 0 & 0 & 0 & 0 & 0\\ 1/2 & 0 & 0 & 0 & 0 & 0 & 0 & 1/2 \end{bmatrix}, \tag{5}$$

$$\rho_{\rm W}=\begin{bmatrix} 0 & 0 & 0 & 0 & 0 & 0 & 0 & 0\\ 0 & 1/3 & 1/3 & 0 & 1/3 & 0 & 0 & 0\\ 0 & 1/3 & 1/3 & 0 & 1/3 & 0 & 0 & 0\\ 0 & 0 & 0 & 0 & 0 & 0 & 0 & 0\\ 0 & 1/3 & 1/3 & 0 & 1/3 & 0 & 0 & 0\\ 0 & 0 & 0 & 0 & 0 & 0 & 0 & 0\\ 0 & 0 & 0 & 0 & 0 & 0 & 0 & 0\\ 0 & 0 & 0 & 0 & 0 & 0 & 0 & 0 \end{bmatrix}. \tag{6}$$

Finally, equation (4) takes the form

$$\rho_{\rm o}=\begin{bmatrix} (1-p)/2 & 0 & 0 & 0 & 0 & 0 & 0 & (1-p)/2\\ 0 & p/3 & p/3 & 0 & p/3 & 0 & 0 & 0\\ 0 & p/3 & p/3 & 0 & p/3 & 0 & 0 & 0\\ 0 & 0 & 0 & 0 & 0 & 0 & 0 & 0\\ 0 & p/3 & p/3 & 0 & p/3 & 0 & 0 & 0\\ 0 & 0 & 0 & 0 & 0 & 0 & 0 & 0\\ 0 & 0 & 0 & 0 & 0 & 0 & 0 & 0\\ (1-p)/2 & 0 & 0 & 0 & 0 & 0 & 0 & (1-p)/2 \end{bmatrix}. \tag{7}$$

Using the above initial density matrix $\rho_{\rm o}$, and time unitary matrix $U(t)$ in Eq. (3), we derive the time evolved state of the system given in Eq. (2) as

$$\rho_{abc}(t)=\begin{bmatrix} (1-p)/2 & 0 & 0 & 0 & 0 & 0 & 0 & -\frac{1}{2}(p-1)X_1\\ 0 & p/3 & pX_2/3 & 0 & pX_3/3 & 0 & 0 & 0\\ 0 & pX_4/3 & p/3 & 0 & pX_5/3 & 0 & 0 & 0\\ 0 & 0 & 0 & 0 & 0 & 0 & 0 & 0\\ 0 & pX_6/3 & pX_7/3 & 0 & p/3 & 0 & 0 & 0\\ 0 & 0 & 0 & 0 & 0 & 0 & 0 & 0\\ 0 & 0 & 0 & 0 & 0 & 0 & 0 & 0\\ -\frac{1}{2}(p-1)X_8 & 0 & 0 & 0 & 0 & 0 & 0 & (1-p)/2 \end{bmatrix}, \tag{8}$$

where

$$\begin{aligned} X_1&=\exp(-2\mathrm{i}t(\mathcal{D}_a+\mathcal{D}_b+\mathcal{D}_c)\mathcal{L}),\\ X_2&=\exp(-2\mathrm{i}t(\mathcal{D}_b-\mathcal{D}_c)\mathcal{L}),\\ X_3&=\exp(-2\mathrm{i}t(\mathcal{D}_a-\mathcal{D}_c)\mathcal{L}),\\ X_4&=\exp(2\mathrm{i}t(\mathcal{D}_b-\mathcal{D}_c)\mathcal{L}),\\ X_5&=\exp(-2\mathrm{i}t(\mathcal{D}_a-\mathcal{D}_b)\mathcal{L}),\\ X_6&=\exp(2\mathrm{i}t(\mathcal{D}_a-\mathcal{D}_c)\mathcal{L}),\\ X_7&=\exp(2\mathrm{i}t(\mathcal{D}_a-\mathcal{D}_b)\mathcal{L}),\\ X_8&=\exp(2\mathrm{i}t(\mathcal{D}_a+\mathcal{D}_b+\mathcal{D}_c)\mathcal{L}). \end{aligned}$$

2.1. The noisy effects and relative influence

In this section, we provide the analysis to derive the final density matrix of the system under relative mixed noise cases. The final density matrix of the considered form is obtained by the average of the phase factors, as illustrated in Ref. [37]. For the first case of making the two qubits exposed to RT and the third to OU noise, the final density matrix is[39]

$$\rho_y(t)=\langle\langle\langle\rho(\mathcal{Q}_a(t),\mathcal{Q}_b(t),\mathcal{Q}_c(t))\rangle\rangle_{\chi_a(t)}\rangle_{\chi_b(t)}\rangle_{\mathcal{Q}_c(t)}, \tag{9}$$

where the explicit form of the above matrix is

$$\rho_y(t)=\begin{bmatrix}
(1-p)/2 & 0 & 0 & 0 & 0 & 0 & 0 & -\frac{1}{2}\mathrm{e}^{-2\beta(t)}(p-1)\mathcal{G}(t)^2\\
0 & p/3 & \frac{p\mathcal{G}(t)^2}{3} & 0 & \frac{1}{3}\mathrm{e}^{-2\beta(t)}p\mathcal{G}(t) & 0 & 0 & 0\\
0 & \frac{p\mathcal{G}(t)^2}{3} & p/3 & 0 & \frac{1}{3}\mathrm{e}^{-2\beta(t)}p\mathcal{G}(t) & 0 & 0 & 0\\
0 & 0 & 0 & 0 & 0 & 0 & 0 & 0\\
0 & \frac{1}{3}\mathrm{e}^{-2\beta(t)}p\mathcal{G}(t) & \frac{1}{3}\mathrm{e}^{-2\beta(t)}p\mathcal{G}(t) & 0 & p/3 & 0 & 0 & 0\\
0 & 0 & 0 & 0 & 0 & 0 & 0 & 0\\
0 & 0 & 0 & 0 & 0 & 0 & 0 & 0\\
-\frac{1}{2}\mathrm{e}^{-2\beta(t)}(p-1)\mathcal{G}(t)^2 & 0 & 0 & 0 & 0 & 0 & 0 & (1-p)/2
\end{bmatrix}. \tag{10}$$

For the second case, imposing OU noise on two qubits and RT noise on the last one, the density matrix is obtained by

$$\rho_x(t)=\langle\langle\langle\rho(\mathcal{Q}_a(t),\mathcal{Q}_b(t),\mathcal{Q}_c(t))\rangle_{\mathcal{Q}_a(t)}\rangle_{\mathcal{Q}_b(t)}\rangle_{\chi_c(t)}, \tag{11}$$

where $\mathcal{Q}_n(t)(\chi_n(t))$ is the phase of the system where $\mathcal{Q}_n(t)/\chi_n(t)=-\imath\int_0^t\mathcal{L}D_n(t)\mathrm{d}t$. Here the first one shows the exposure of OU noise phase while the second $\chi_n(t)$ shows the application of RT noise phase. The explicit form of the above matrix reads as

$$\rho_x(t)=\begin{bmatrix}
(1-p)/2 & 0 & 0 & 0 & 0 & 0 & 0 & -\frac{1}{2}\mathrm{e}^{-4\beta(t)}\mathcal{G}(t)(p-1)\\
0 & p/3 & \frac{1}{3}\mathrm{e}^{-2\beta(t)}\mathcal{G}(t)p & 0 & \frac{1}{3}\mathrm{e}^{-2\beta(t)}\mathcal{G}(t)p & 0 & 0 & 0\\
0 & \frac{1}{3}\mathrm{e}^{-2\beta(t)}\mathcal{G}(t)p & p/3 & 0 & \frac{1}{3}\mathrm{e}^{-4\beta(t)}p & 0 & 0 & 0\\
0 & 0 & 0 & 0 & 0 & 0 & 0 & 0\\
0 & \frac{1}{3}\mathrm{e}^{-2\beta(t)}\mathcal{G}(t)p & \frac{1}{3}\mathrm{e}^{-4\beta(t)}p & 0 & p/3 & 0 & 0 & 0\\
0 & 0 & 0 & 0 & 0 & 0 & 0 & 0\\
0 & 0 & 0 & 0 & 0 & 0 & 0 & 0\\
-\frac{1}{2}\mathrm{e}^{-4\beta(t)}\mathcal{G}(t)(p-1) & 0 & 0 & 0 & 0 & 0 & 0 & (1-p)/2
\end{bmatrix}, \tag{12}$$

where $\beta(t)$ induces the OU noise while $\mathcal{G}(t)$ induces RT noise.

Next, we address the application of OU noise. A stochastic mathematical technique known as the OU process is applied in both the physical sciences and finance. A huge Brownian particle's velocity when it comes into contact with friction is modeled in physics. One of the essential components of several quantum mechanical procedures that result in non-classical characteristics decay, has been shown to be OU noise. A static Gaussian Markov operation underlies the OU method.[41,43,43] OU noise has been thoroughly investigated for the cases of multi-qubit, single-qutrit, and combined qubit-qutrit configurations, where it is obvious that each configuration exhibit invariant dynamics and decay.[44–47] The three-qubit GHZ state's dynamical map, which was initially created in the state ρ_0, is revealed in the current scenario. In order to evaluate the non-positive effects of OU noise, a Gaussian process ($\langle\mathcal{CF}(t)\rangle=0$) with zero-mean is considered which may be used to represent the classical field $\mathcal{CF}(t)$. Following is the auto correlation function of the OU noise[37]

$$\nu(g,t-t')=g(\exp[-g|t-t'|]1/2. \tag{13}$$

To demonstrate the influence of the respective noise, we present the β-equation as[41]

$$\beta(t)=\int_0^t\int_0^t L(F-F')\mathrm{d}F\,\mathrm{d}F'. \tag{14}$$

We insert Eq. (13) in Eq. (14) and finally get[41,42]

$$\beta(t)=(gt+\exp[-gt]-1)1/g, \tag{15}$$

where g denotes the inverse auto-correlation time, regulating the memory characteristics of the field.

A bistable frequency oscillator produces the RTN noise, which has been used to define enormous physical processes in semiconductor apparatus with small dimensions[48] and may or may not be Markovian. In solid-state, magnetic systems as well as in superconducting qubits, RTN noise is the main contributor to environmental decoherence. Additionally, it has a big impact on colored noise production.[49–51] It is needed to compute $\langle i\mathrm{e}^{\imath m\mathcal{Q}(t)}\rangle$, terms of average type to determine how noise affects the dynamics of the system[52,53] as

$$\begin{aligned}\mathcal{G}(t) &= \langle\cos(m\mathcal{Q}(t))\rangle\\ &= \begin{cases}\mathrm{e}^{-\Gamma t}[\cosh(\delta_{m\gamma}t)+\frac{\Gamma}{\delta_{m\gamma}}\sinh(\delta_{m\gamma}t)], & \Gamma>m\gamma,\\ \mathrm{e}^{-\Gamma t}[\cos(\delta_{m\gamma}t)+\frac{\Gamma}{\delta_{m\gamma}}\sin(\delta_{m\gamma}t)], & \Gamma<m\gamma,\end{cases}\\ \langle\sin(m\mathcal{Q}(t))\rangle &= 0,\end{aligned} \tag{16}$$

where $\delta_{m\gamma}=\sqrt{|\Gamma^2-(m\gamma)^2|}$ and m is an integer representing the harmonic order of the oscillatory process.

2.2. Coherence and entanglement measurement

We start by examining coherence, entanglement, and purity in the considered configuration stated above.

2.2.1. The ℓ_1-norm of coherence

The ℓ_1-norm is a reliable coherence monotone and a coherence criterion.[21] Besides, ℓ_1-norm coherence for a two-qubit state $\rho=\sum_{u,v}\rho_{uv}|u\rangle\langle v|$ is the sum of all off-diagonal

entries as

$$LC(t) = \sum_{u \neq v} |\rho_{u,v}|, \tag{17}$$

where $|\rho_{u,v}|$ is the density matrix element's absolute values.

2.2.2. Entanglement witness meassure

Experimental methods for detecting multipartite or bipartite entanglement can be employed with observables called entanglement witnesses (EWs).[54] Separable states, biseparable states, W-class states, and GHZ-class states are the four different varieties of three-qubit mixed states.[55] Each class comprises variations of the classes that came before it. EWs are capable of helping show what category a state belonged to, and in this case, they will be utilized to verify if a state matches the true tripartite entanglement of the GHZ-class, which is described as, $\mathcal{E}s_1 = \frac{1}{2}I_8 - \rho_0$, $\mathcal{E}s_2 = \frac{2}{3}I_8 - \rho_0$, and $\mathcal{E}s_3 = \frac{3}{4}I_8 - \rho_0$. The EWs for any entangled state take the form[56]

$$EW(t) = -\mathrm{Tr}[\mathcal{E}s_n \rho(t)], \tag{18}$$

where $\mathcal{E}s_n$ are the EWs operator, with $n = 1,2,3$. The condition $EW(t) > 0$ signifies the entanglement regime , $EW(t) = 0$ means the full separability of the state. The non-positive outcomes, *i.e.*, $EW(t) < 0$ do not fully ensure the full separability of the state.

2.2.3. Purity

To evaluate how much the system remains coherent, and pure, one may employ purity measure.[57] For a density matrix $\rho(t)$, purity measure is computed by

$$P(t) = \mathrm{Tr}[\rho(t)^2], \tag{19}$$

with q dimensional system, purity ranges as $1/q \leq P(t) \leq 1$, where at the lower bound $(1/q)$, the system is decoherent/unpure and for the higher bound, the system is assumed completely pure.[58]

3. Entanglement, coherence, and purity dynamical analysis

The major outcomes for the configuration obtained exposing the coherence, entanglement, and purity evolution using the measures in Eqs. (17), (18), and (19). Note that for the dephasing to be included, we define two different cases: when two qubits are coupled with two RT noisy and one qubit to interact with OU noisy channels (Eq. (9)) and so the opposite of this configuration (Eq. (11)).

3.1. First case: The influence of one OU and two RT noisy channels

Here, the time evolution of coherence, entanglement, and purity in the GHZ-like and W-like states while exposing one qubit is exposed to OU and two qubits with RT noisy channels.

Figure 1 shows the dynamics of quantum characteristics such as coherence (a), entanglement witness (b), and purity (c) for a system of three qubits, initially prepared as GHZ-like and W-like states. Note that we have coupled two qubits with RT noise and one qubit to interact with OU noise. At the onset, the W-like state remained more coherent than the GHZ-like state, as the initial coherence function values were greater than that observed for the GHZ-like state. Besides, both states remained initially maximally entangled and pure, which contradicts the results obtained for the coherence function.

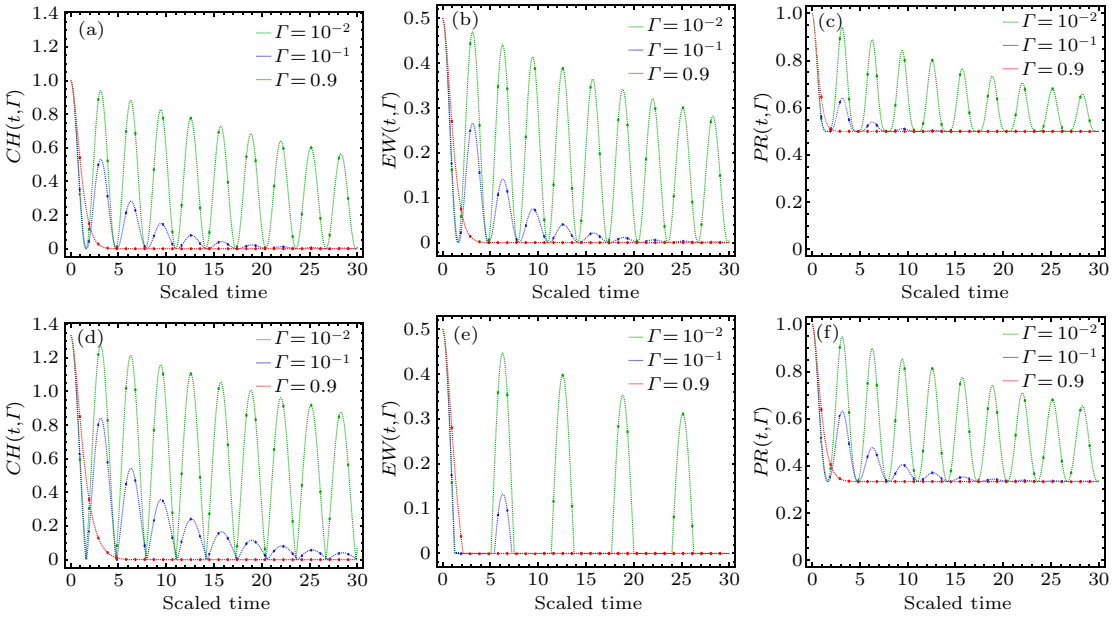


Fig. 1. Dynamics of (a) coherence, (b) entanglement, and (c) purity when dependent upon parameter Γ against scaled time in three-qubit GHZ state (upper panel) and W-state (bottom panel) influenced by one OU noisy and two RT noisy channels.

With time, all three functions remain to decrease because of the action of the dephasing channels on the state and eventually, the coherence, entanglement, and purity in the state seem to vanish. As coherence vanishes more quickly in the GHZ-like state while comparing to the W-like state. However, the opposite occurs for the entanglement witness and purity function, where the GHZ-like state remains highly consistent for entanglement preservation and avoids mixedness. Hence, the GHZ-like state is a good resource for preserving entanglement and pureness with regard to W-like state under the influence of local dephasing channels. Besides, the dynamics of the quantum correlations and purity of the state suffered reaped sudden deaths and births. This means that the states at intervals become completely decoherent, disentangled and mixed. But because the current channels allow for the state-field information interchange, therefore the state regains the loss of coherence, entanglement and purity. However, the fact cannot be ignored that some portion of the coherence, entanglement and purity is always lost after the sudden death. Here, we mainly characterize the coherence, entanglement and purity functions by the RT noise parameter Γ. It can be seen the increasing values of Γ inversely affect the preservation of the three-qubits correlations. Like, the reduced Γ strength allows for the greater preservation of the coherence, entanglement and purity, while the complete opposing occurs against the greater values of the parameter. It is noteworthy that for the lower Γ values, the coherence, entanglement and purity functions shows larger sudden death and birth revivals, while when $\Gamma \to 1$, the dynamics of the three-qubits correlations dominantly become Markovian. Hence, the Markovian/non-Markovian character of the current classical dephasing channels is highly controlled by the parameter of Γ.

Figure 2 shows the coherence, entanglement, and purity of three qubits GHZ-like state and W-like state when one qubit is linked with OU noisy dephasing channel and two qubits with RT noisy dephasing channels. In the current case, we specifically want to disclose what happens to the non classical features of the state when exposed to the classical channels. For this reason, we have majorly defined the ℓ_1 norm of coherence, entanglement witness and purity of the GHZ- and W-like states. In agreement with Fig. 1, the coherence magnitude in the W-like remains greater than that is observed in the GHZ-like state initially. In the case of entanglement and purity, the GHZ-like and W-like states remain equivalent. After the onset, the initial degree of quantum features in the state reduce non-monotonically depending upon the strength of the associated dephasing parameter. For example, for the higher g values, the coherence, entanglement, and purity functions show a quicker decline while the opposite has been witnessed for the lower g values. Besides Γ, the fluctuating dynamical map of the qubit correlations is strongly influenced by the strength of g. As seen for the lower g values, a dominant non-monotonic dynamical map is observed for each function and *vice versa*. The existence of sudden death and births ensure the transitions of the GHZ-like and W-like states from the classical product regimes to the non local superimposed domains. This is compared to the case when the tripartite correlations functions were defined primarily by parameter Γ, the present case shows a greater decline in coherence, entanglement, and purity. Hence, it suggests that the characterization of the tripartite correlations also depends upon the parameter which primarily owns it.

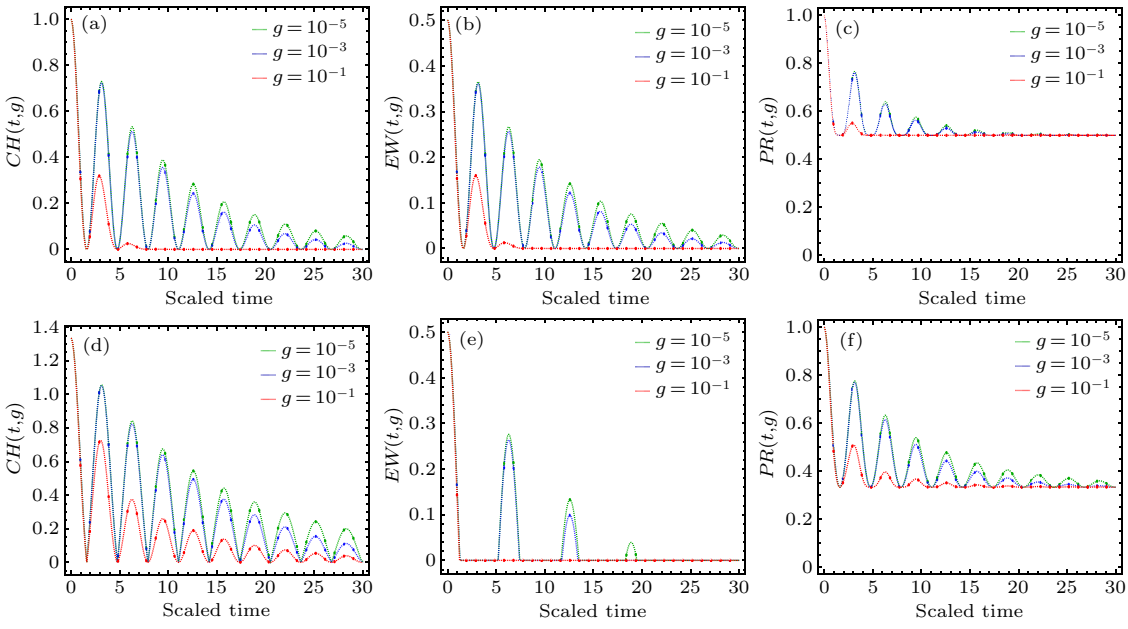


Fig. 2. Dynamics of (a) coherence, (b) entanglement, and (c) purity when dependent upon parameter g against scaled time in three-qubit GHZ state (upper panel) and W-state (bottom panel) influenced by one OU noisy and two RT noisy channels.

3.2. Second case: The influence of one RT and two OU noisy channels

When two qubits are connected to OU noisy channels and one qubit interacts with the RT noisy channel, we discuss some given quantum features in the GHZ- and W-like states.

The dynamics of the coherence, entanglement, and purity in the GHZ- and W-like states when subjected to two OU and a single RT noise is shown in Fig. 3. Both the states have a similar amount of coherence, entanglement, and purity as detected in Figs. 1 and 2, hence, agree with the previous results. Besides, the fact that the initial coherence value remains greater in the W-like state than the opponent one remained valid. On the contrary, the entanglement and purity values at the onset remain the same. After the start of the interaction, the coherence, entanglement, and purity functions suffer losses because of the action of the dephasing channels. The behavioral dynamics of the GHZ-like and W-like states remain more favorable when two OU noisy and one RT noisy channels are used, compared to the opposite case explored in Figs. 1 and 2. As seen for the lower Γ values, the coherence, entanglement, and purity functions remain more preserved than that observed previously. However, for the increased Γ values, the current configuration not remained optimal for the quantum features preservation of the states. For example, one can

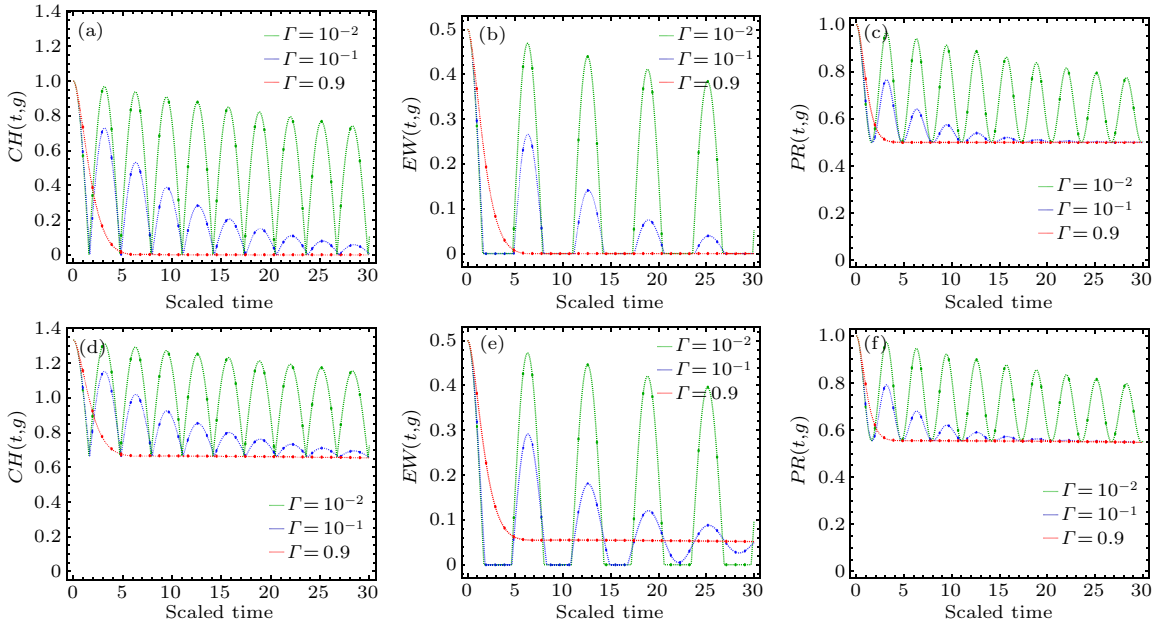


Fig. 3. Dynamics of (a) coherence, (b) entanglement, and (c) purity when dependent upon parameter Γ against scaled time in three-qubit GHZ state (upper panel) and W-state (bottom panel) influenced by two OU noisy channels and one RT noisy channel.

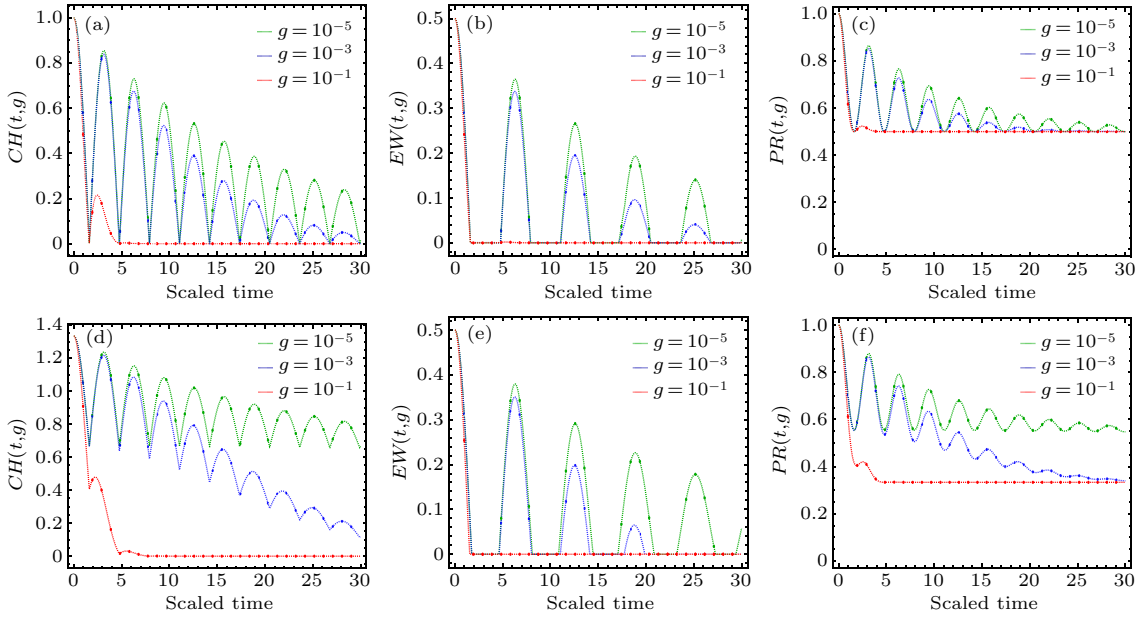


Fig. 4. Dynamics of (a) coherence, (b) entanglement, and (c) purity when dependent upon parameter g against scaled time in three-qubit GHZ state (upper panel) and W-state (bottom panel) influenced two OU noisy channels and one RT noisy channel.

see that for $\Gamma = 0.9$, all the three-qubit correlation quantifiers suffer a quicker decay. Besides this, the lower Γ values highly supported the non-monotonic behavioral dynamical map, while the opposite happen when Γ is raised to higher values. In agreement with previous results, sudden death/birth oscillations are witnessed, depicting interchange of information between the state and field. This also can be disclosed as a phenomenon needed for the inter transitions of the free classical and quantum resource states into each other. The major difference we witnessed between the two cases; when two OU and one RT noisy channel are employed with the one under study here, is the between the rate of sudden death and births, preservation of non-local characteristics and amplitude of oscillation. Hence, classical channels and the associated decaying effects are mainly concentrated on the type of dephasing noise involved. In comparisons, it is interesting to notice that the W-like state compared to the GHZ-like state has shown highly improved preservation of quantum correlations. This is in complete contradiction to the case when two RT and one OU noise channels are employed, as shown in Figs. 1 and 2.

The behavioral dynamics of coherence, entanglement and purity in a three-qubit state when coupled to two OU and one RT noisy dephasing channels is shown in Fig. 4. The current results are obtained when the coherence, entanglement, and purity functions are characterized primarily by the OU noise parameter g. Initially, both states have equivalent maximal entanglement and purity, unlike the unequal values of coherence. As seen that the W-like state remained more coherent initially than the GHZ-like state. With time, all three functions show a decline, showing the presence of dephasing induced because of the application of the classical channels. The decay induced in the states remained very dissimilar. In the GHZ state, the decay remained symmetrical and the coherence, entanglement, and purity functions declined with a regular pattern. However, regarding W-like system, some irregular decay has been witnessed in coherence and purity, except for the entanglement. It is interesting to find that for the lower and higher g values, the W-type state remained more preserved for quantum correlations compared to the GHZ-like state. However, the rate of revivals remains more prominent in the GHZ-like state compared to the W-like state. This implies that the interchange of data between the system and fields remain more dominant as compared to the interaction between the W-like state and associated fields. We find that the application of two OU noisy and one RT noisy channels remained more favorable and declined primarily characterized by the parameter Γ (Fig. 3) when compared to that of g (Fig. 4).

3.3. The entropic uncertainty measurement

Not only in theoretical sense but quantum memory assisted entropic uncertainty (QMA-EU) relations also have practical implications in quantum technologies and quantum information processing. They shed light on the fundamental limits and advantages of using quantum resources to improve precision and control in quantum systems, and essential for advancing the field of quantum related studies.[62] Besides, to investigate, consider two players, namely, Alice and Bob as Alice holds two qubits and Bob holds one qubit. Next, a qubit of the optimal quantum state designed priory by Bob is received by Alice. The first player Alice has to decide one between the measurements received and again send it to the other player. The outcome uncertainty can now be tailored low utilizing the Bob's results information.[59] In this regard, the uncertainty standard deviation when $\mathcal{C}$ and $\mathcal{D}$ being two observables, where these obsevables are $C = \sigma_x \otimes \sigma_x$, $D = \sigma_z \otimes \sigma_z$ becomes as $\Delta\mathcal{C}\Delta\mathcal{D} \geq 1/2|\langle[\mathcal{C}, \mathcal{D}]\rangle|$.[59]

Deutsch has provided the entropic uncertainty formula for every couple of observables, which is depicted in the formula above, as an alternative to using the standard deviation to characterise uncertainty.[63] Maassen and Uffink developed a more precise entropic uncertainty formulation that utilises Deutsch's approach, which is denoted as $S(\mathcal{C}) + S(\mathcal{D}) \geq \log_2 c(\mathcal{C};\mathcal{D})$,[60] where $S(K)(K = \mathcal{C}, \mathcal{D})$ is the Shannon entropy having the associated probability distribution for observable K while $c(\mathcal{C};\mathcal{D}) = \max_{a,\, b} |\langle\psi|\mathcal{Q}\rangle|^2$ remains the maximized reinforcement of the two eigenvectors ψ and $\mathcal{Q}$. Berta *et al.* offered an improved description that took into account the entropic uncertainty relations in composite systems and provided an entropic uncertainty relation that was helped by quantum memory.[61] As a result, with a tighter restriction, the QMA-EU for the subsystem A is replicated in accordance with quantum memory B. Moreever, entropic uncertainty reflects quantum correlations and helps quantify their robustness under noise.[64]

$$S(\mathcal{C}|B) + S(\mathcal{D}|B) \geq S(A|B) - \log_2 c(\mathcal{C};\mathcal{D})), \tag{20}$$

where $S(\mathcal{C}|B) = S(\rho_{\mathcal{C}B}) - S(\rho_B)$ is the conditional entropy after the unilateral measurement on $\mathcal{C}$ with regard to subsystem A. In our case, we emphasize measuring the left-hand side of the uncertainty relations given in Eq. (20).

In Fig. 5, we disclosed generation of entropic uncertainty considering the three-qubit system under local fields (a) [(upper panel) when two of the qubits are driven by the OU and one by RT noise, (b) and the opposite configuration of (lower panel)] driven by joint noisy sources. The degree of uncertainty has been shown for varying purity values of the state against time. One can easily find that when two qubits are driven by the OU noise, the generation rate of the entropic uncertainty remains sufficiently high (upper case). As can be seen that the state has been witnessed with high entropic uncertainty compared to the case when two qubits are coupled with RT noise. However, it should be noted that we have set $g = 1$, and $\Gamma = 0.9$ [cases (a) and (c)]. In comparisons, when

$g = \Gamma = 0.1$ [cases (b) and (d)], the state exhibits lower entropic uncertainity generation when the two qubits are coupled with OU noise, as can be seen that the higher uncertainty regimes are archived latter. Besides, the mixture state remains completely free of the entropic uncertainty at the onset, however, only when $p \in \{0,1\}$. It is clear that at the onset the maximum entropic uncertainty occurs at $p = 0.5$. With time, the three-qubit mixture state loses the entropic uncertainty-free regime quickly at $p = 0$ compared to the case of $p = 1$. Hence, suggesting that the state remains more tolerant to the external noisy effects at $p = 1$ comparatively.

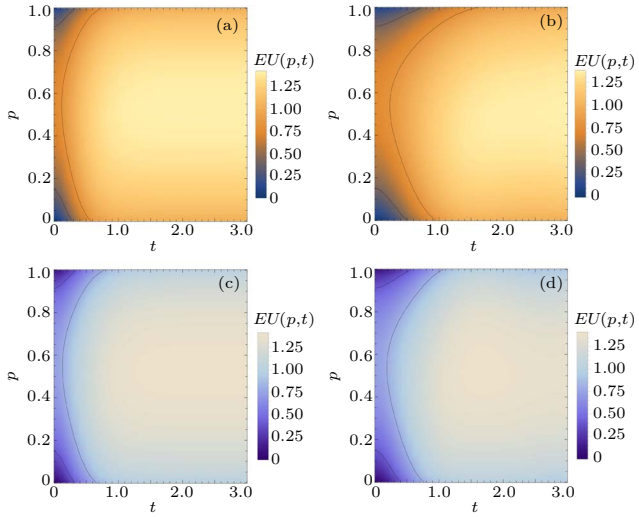


Fig. 5. Dynamics of entropic uncertainty in the three-qubit mixture state when influenced by two OU and one RT noisy channels (upper panel) and when by two RT and one OU noisy channels (lower panel) with $\Gamma = 0.9$ and $g = 1$ [(a), (c)] while $\Gamma = 10^{-1}$ and $g = 10^{-1}$ [(b) and (d)].

3.4. Fidelity measurement

In this section, we cover the extent to which the state remains distinguished from that considered initially. Let us consider the original state to be $\sigma = |GHZ\rangle\langle GHZ|$ with $|GHZ\rangle = 1/\sqrt{2}(|000\rangle + |111\rangle)$. Now consider the state to be evaluated as $\rho_j(t)$ given in Eqs. (9) and (11) with $j \in \{x,y\}$. The fidelity between the evolved three-qubit state $\rho_j(t)$ and the reference GHZ state $\sigma = |GHZ\rangle\langle GHZ|$ is quantified using the standard fidelity measure, given by

$$F(\rho_j(t),\sigma) = \left(\mathrm{Tr}\left[\sqrt{\sqrt{\rho_j(t)}\,\sigma\,\sqrt{\rho_j(t)}}\right]\right)^2. \qquad (21)$$

Note that the fidelity remains maximum at $p = 1$ and is completely lost at $p = 0$ by the state. Any value between the upper and lower bound will indicate the associated amount of fidelity between the states.

The time evolution of the three-qubit state's fidelity is examined under the two conditional environments: (i) when two of the qubits are driven by OU and one by RT noise, (ii) and the opposite configuration of panel (a) in Fig. 6. We have considered density statistical ensemble σ comprising the three qubit $|GHZ\rangle$ state with maximal entanglement as the reference one. The fidelity dynamics has been then studied for the states given in Eqs. (9) and (11) compared to σ. In this regard, figure 6(a) shows that the fidelity measurement outcome is maximum at $p = 0$ of the three-qubit mixture state at the onset. For $p \neq 0$, the fidelity decreases correspondingly at the very initial level. As the interaction between the channels and state in the first case (i) evolves, the relative fidelity suffers a sudden decrease, which is common for all fidelity levels relative to any p value. At $p = 0$, the state exhibits deeper sudden decreases and retrieval of the fidelity, however, finds stabilization at the highest level as compared to all other p values. Therefore, this suggests the best fidelity achievement for the three-qubit mixture state at $p = 0$. For the second case (ii), when two RT noisy channels are enforced over two qubits and OU over the last one, the onset values seem comparable to that found in case (i). However, the rest of the dynamical outlook of the fidelity remains completely different. For example, the oscillatory rate is enough high and the pattern is more consistent compared to that in case (i). In comparison, the fidelity revivals exhibit a longer time in case (ii) compared to case (i). Hence predicting the long-lasting exchange of information between the channels and state.

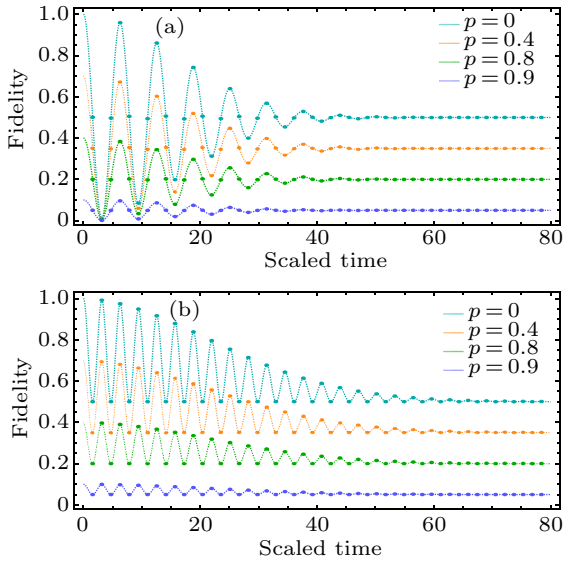


Fig. 6. Dynamics of fidelity in the three-qubit mixture state when influenced by two OU and one RT noisy channels (upper panel) and when by two RT and one OU noisy channels (lower panel) with $g/\Gamma = 1$.

4. Conclusion

We have investigated the dynamics of quantum features such as coherence, entanglement, purity, entropic uncertainty, and fidelity in two different three-qubit class states; the GHZ- and W-like states. Both states are further subjected to mixed classical dephasing channels influenced by the OU and RT noises in two different configurations. In the first systematic configuration, two independent RT and one OU noisy channels are employed while, the opposite of the first configuration has

been adopted. Next, we have used ℓ_1 norm of coherence, entanglement witness and purity measures to find the degree of coherence, entanglement, and purity under the effects of classical dephasing. Finally, all three quantifiers are characterized by the noise parameters to see their different impacts.

We found that the mixed OU and RT noisy channels induce a non-monotonic decay in the three-qubit coherence, entanglement, and purity. The sudden death and birth events in the three-qubit correlations remained very evident under the current classical dephasing effects. However, the non-monotonic dynamical maps of the coherence, entanglement, and purity are more evident when the noise parameters are kept minimal. The optimal configuration for the longer and larger quantum correlations and purity preservation, we found, was when two OU and RT noisy channels ate deployed. Besides, the GHZ-like state has been found less coherent initially, in comparison. However, the overall performance of the GHZ- and W-like states depends upon the configuration of the noise. For example, when two RT and one OU noisy channels are applied, the GHZ-like state has performed well in preserving quantum correlations. The W-like state remained well-preserved for the quantum correlations when two of its qubits were coupled with OU and one qubit with RT noise. In addition, the entropic uncertainty measurement suggests that the state exhibited the least uncertainty when the three-qubit mixture is set at $p = 1$. Besides, the fidelity measurement suggests that the state remains nearly the indistinguishably similar at $p = 0$ and 1. Hence, the three-qubit states have different capacities and responses toward enduring the classical dephasing effects. Most importantly, we found that understanding the influence of these noisy channels is essential for assessing the robustness of quantum systems in practical applications of the quantum computing protocols, as it provides a variety of controlled parameters and can allow for longer quantum correlations preservation.

Acknowledgements

Project supported by the Fund from Guangdong Provincial Quantum Science Strategic Initiative (Grant Nos. GDZX2505001 and GDZX2303009), the National Natural Science Foundation of China (Grant No. 62273154), and the TCL Science and Technology Innovation Fund (Grant No. 20242062).

References

[1] Nielsen M A and Chuang I L 2000 *Quantum Computation and Quantum Information* (Cambridge: Cambridge University Press)
[2] Horodecki R, Horodecki P, Horodecki M and Horodecki K 2009 *Rev. Mod. Phys.* **81** 865
[3] Corrected entry: Breuer H P and Petruccione F 2002 *The Theory of Open Quantum Systems* (Oxford: Oxford University Press)
[4] Hornberger K 2009 *Introduction to Decoherence Theory in Entanglement and Decoherence*, eds. A Buchleitner, C Viviescas and M Tiersch (Berlin, Heidelberg: Springer) pp. 221–276
[5] Hein M, Dür W and Briegel H J 2005 *Phys. Rev. A* **71** 032350
[6] Dajka J and Luczka J 2010 *Phys. Rev. A* **82** 012341
[7] Ban M 2012 *Phys. Rev. A* **85** 042110
[8] Head-Marsden K, Flick J, Ciccarino C J and Narang P 2020 *Chem. Rev.* **121** 3061
[9] Dür W, Vidal G and Cirac J I 2000 *Phys. Rev. A* **62** 062314
[10] Gao X, Ma Z and Qin G 2019 *J. Phys. A: Math. Theor.* **52** 475301
[11] Rahman A U, Haddadi S, Javed M, Kenfack L T and Ullah A 2022 *Quantum Inf. Process.* **21** 368
[12] Gottesman D 1998 *Phys. Rev. A* **57** 127
[13] Li T, Luo S and Li Y 2012 *Phys. Rev. A* **86** 032334
[14] SenDe A and Sen U 2010 *Phys. Rev. A* **81** 012308
[15] Javed M, Salim S, Said S, Shah K and Ur Rahman A 2024 *Laser Phys.* **34** 035202
[16] Streltsov A, Singh U, Dhar H S, Bera M N and Adesso G 2015 *Phys. Rev. Lett.* **114** 210401
[17] Yuan X, Zhou H, Cao Z and Ma X 2016 *Sci. Rep.* **6** 29260
[18] Bromley T R, Cianciaruso M and Adesso G 2016 *Phys. Rev. A* **93** 060303
[19] Wang Y T, Tang J S, Huang Y F, Li C F and Guo G C 2020 *Sci. China-Phys. Mech. Astron.* **63** 230322
[20] Hu M L, Hu X, Wang J C, Peng Y, Zhang Y R and Fan H 2018 *Phys. Rep.* **762–764** 1
[21] Baumgratz T, Cramer M and Plenio M B 2014 *Phys. Rev. Lett.* **113** 140401
[22] Streltsov A, Adesso G and Plenio M B 2017 *Rev. Mod. Phys.* **89** 041003
[23] Corrected entry: Greenberger D M, Horne M A and Zeilinger A 1989 *Going Beyond Bell's Theorem in Bell's Theorem, Quantum Theory and Conceptions of the Universe*, ed. Kafatos M (Dordrecht: Springer) pp. 69–72
[24] Dür W, Vidal G and Cirac J I 2000 *Phys. Rev. A* **62** 062314
[25] Harraz S, Cong S and Nieto J J 2022 *Int. J. Quantum Inform.* **20** 2250007
[26] Horodecki R, Horodecki P, Horodecki M and Horodecki K 2009 *Rev. Mod. Phys.* **81** 865
[27] Cunha M, Fonseca A and Silva E O 2019 *Universe* **5** 209
[28] Vidal G 2002 *J. Mod. Opt.* **49** 355
[29] Štelmachovič P and Bužek V 2004 *Phys. Rev. A* **70** 032313
[30] Sen A, Sen U and Lewenstein M 2007 *Phys. Rev. A* **72** 052319
[31] Corrected entry: Nielsen M A and Chuang I L 2010 *Quantum Computation and Quantum Information: 10th Anniversary Edition* (Cambridge: Cambridge University Press)
[32] Corrected entry: Breuer H P and Petruccione F 2002 *The Theory of Open Quantum Systems* (Oxford: Oxford University Press)
[33] Yu T and Eberly J H 2004 *Phys. Rev. Lett.* **93** 140404
[34] Benedetti C and Paris M G A 2014 *Phys. Rev. A* **89** 012114
[35] Paladino E, Galperin Y M, Falci G and Altshuler B L 2014 *Rev. Mod. Phys.* **86** 361
[36] Volpe G and Wehr J 2016 *Rep. Prog. Phys.* **79** 053901
[37] Rahman A U, Javed M, Ji Z and Ullah A 2021 *J. Phys. A: Math. Theor.* **55** 025305
[38] Benabdallah F, Rahman A U, Haddadi S and Daoud M 2022 *Phys. Rev. E* **106** 034122
[39] Rahman A U, Noman M, Javed M, Luo M X and Ullah A 2021 *Quantum Inf. Process.* **20** 290
[40] Rahman A U, Haddadi S, Javed M, Kenfack L T and Ullah A 2022 *Quantum Inf. Process.* **21** 368
[41] Rossi M A C, Benedetti C and Paris M G A 2014 *Int. J. Quantum Inf.* **12** 1560003
[42] Kenfack L T, *et al.* 2017 *Physica B* **511** 123
[43] Benedetti C and Paris M G A 2014 *Phys. Lett. A* **378** 2495
[44] Corrected entry: Ferrante P, Nicolosi S, Scaccianoce G and Rizzo G 2008 arXiv: 0804.0365 [quant-ph]
[45] Mirza I M 2015 *J. Mod. Opt.* **62** 1048
[46] del Pino J, Feist J and Garcia-Vidal F J 2015 *New J. Phys.* **17** 053040
[47] Buchhold M, Strack P, Sachdev S and Diehl S 2013 *Phys. Rev. A* **87** 063622
[48] Corrected entry: Spagnolo B, Guarcello C, Magazzu L, Carollo A, Adorno D P and Valenti D 2017 *Entropy* **19** 20
[49] Hung K K, Ko P K, Hu C and Cheng Y C 1990 *IEEE Electron Device Lett.* **11** 90
[50] Uren M J, Day D J and Kirton M 1985 *Appl. Phys. Lett.* **47** 1195

[51] Kenfack L T, Tchoffo M, Jipdi M N, Fuoukeng G C and Fai L C 2018 *J. Phys. Commun.* **2** 055011
[52] Corrected entry: van Zelst S J, Fani Sani M, Ostovar A, Conforti R and La Rosa M 2018 *Filtering Spurious Events from Event Streams of Business Processes in Advanced Information Systems Engineering* (CAiSE 2018), eds. J Krogstie and H Reijers *Lecture Notes in Computer Science* 10816 (Cham: Springer) pp. 35–52
[53] Marcuzzi M, Schick J, Olmos B and Lesanovsky I 2014 *J. Phys. A: Math. Theor.* **47** 482001
[54] Chruściński D and Sarbicki G 2014 *J. Phys. A: Math. Theor.* **47** 483001
[55] Acín A, Bruß D, Lewenstein M and Sanpera A 2001 *Phys. Rev. Lett.* **87** 040401
[56] Branciard C, Rosset D, Liang Y C and Gisin N 2013 *Phys. Rev. Lett.* **110** 060405
[57] Schlosshauer M 2019 *Phys. Rep.* **831** 1
[58] Serafini A, Paris M G, Illuminati F and De Siena S 2005 *J. Opt. B: Quantum Semiclassical Opt.* **7** R19
[59] Ming F, Wang D, Fan X G, Shi W N, Ye L and Chen J L 2020 *Phys. Rev. A* **102** 012206
[60] Maassen H and Uffink J B 1988 *Phys. Rev. Lett.* **60** 1103
[61] Berta M, Christandl M, Colbeck R, Renes J M and Renner R 2010 *Nat. Phys.* **6** 659
[62] Bera M N, Prabhu R, Pati A K, SenDe A and Sen U 2012 *Phys. Rev. A* **86** 042105
[63] Recommended corrected entry: Hu M L and Fan H 2013 *Phys. Rev. A* **87** 022314
[64] Pramanik T, Chowdhury P and Majumdar A S 2013 *Phys. Rev. A* **88** 014105